Published in final edited form as:
Res Microbiol. 2014 ; 165(6): 429–438. doi:10.1016/j.resmic.2014.04.005.

PdhR, the Pyruvate Dehydrogenase Repressor, Does not Regulate Lipoic Acid Synthesis

Youjun Feng[a,b,c] and **John E. Cronan**[b,c,*]

[a]Collaborative Innovation Center for Diagnosis and Treatment of Infectious Diseases & State Key Laboratory for Diagnosis and Treatment of Infectious Disease, First Affiliated Hospita, Zhejiang University College of Medicine, Hangzhou, Zhejiang 310058, P.R. China

[b]Department of Medical Microbiology and Parasitology, Zhejiang University College of Medicine, Hangzhou, Zhejiang 310058, P.R. China

[c]Department of Microbiology, University of Illinois at Urbana-Champaign, IL 61801, USA

[d]Department of Biochemistry, University of Illinois at Urbana-Champaign, IL 61801, USA

Abstract

Lipoic acid is a covalently-bound enzyme cofactor required for central metabolism all three domains of life. In the last 20 years the pathway of lipoic acid synthesis and metabolism has been established in *Escherichia coli.* Expression of the genes of the lipoic acid biosynthesis pathway was believed to be constitutive. However, in 2010 Kaleta and coworkers (BMC Syst. Biol. 4:116) predicted a binding site for the pyruvate dehydrogenase operon repressor, PdhR (referred to *lipA* site 1) upstream of *lipA*, the gene encoding lipoic acid synthase and concluded that PdhR regulates *lipA* transcription. We report *in vivo* and *in vitro* evidence that *lipA* is not controlled by PdhR and that the putative regulatory site deduced by the prior workers is nonfunctional and physiologically irrelevant. *E. coli* PdhR was purified to homogeneity and used for electrophoretic mobility shift assays. The *lipA* site 1 of Kaleta and coworkers failed to bind PdhR. The binding detected by these workers is due to another site (*lipA* site 3) located far upstream of the *lipA* promoter. Relative to the canonical PdhR binding site *lipA* site 3 is a half-palindrome and as expected had only weak PdhR binding ability. Manipulation of *lipA* site 3 to construct a palindrome gave significantly enhanced PdhR binding affinity. The native *lipA* promoter and the version carrying the artificial *lipA3* palindrome were transcriptionally fused to a LacZ reporter gene to directly assay *lipA* expression. Deletion of *pdhR* gave no significant change in *lipA* promoter-driven β-galactosidase activity with either the native or constructed palindrome upstream sequences, indicating that PdhR plays no physiological role in regulation of *lipA* expression.

To whom correspondence should be addressed: Dept. of Microbiology, B103, Chemical and Life Sciences Laboratory, 601 S. Goodwin Ave., Urbana, IL 61801. Tel.: 217-333-7919; Fax: 217-244-6697; j-cronan@life.uiuc.edu.

Keywords

PdhR; LipA. Lipoic acid; pyruvate dehydrogenase; 2-oxoglutarate dehydrogenase; Electrophoretic mobility shift assays (EMSA)

1. Introduction

Recently, it was reported that expression of *lipA*, the gene encoding the Fe-S cluster protein that catalyzes insertion of the two sulfur atoms of the key metabolic cofactor, lipoic acid, is repressed by PdhR, the pyruvate-sensitive repressor of the pyruvate dehydrogenase *pdhR aceEF* operon [24]. This report was based on DNA sequence motifs, unspecified microarray data obtained from a central database and electromobility shift analyses (EMSAs) [24]. However, PdhR repression of *lipA* expression seemed both redundant and physiologically problematical to us. The redundancy arises because PdhR already regulates synthesis of AceF, the pyruvate dehydrogenase (PDH) subunit that must be modified by attachment of lipoate for activity of the enzyme complex [5, 6]. The AceF supply necessarily limits the amount of LipA needed because upon modification it becomes the substrate for the LipA-catalyzed sulfur atom insertions. AceF is modified by transfer of an octanoyl group by LipB, the octanoyl transferase that catalysis formation of an amide link between octanoic acid (derived from the octanoyl-acyl carrier protein of fatty acid synthesis) and the ε-amino groups of specific lysine residues present on well-conserved protein domains called lipoyl domains [5, 6]. LipA then inserts the sulfur atoms into the AceF-bound octanoyl group. Hence, unlike other covalently-attached coenzymes (e.g., biotin) which are assembled and then attached, lipoic acid is assembled on its cognate proteins [5, 6]. Hence, lipoate synthesis is hardwired to the supply of octanoylated acceptor proteins (e.g., octanoylated AceF) and therefore cannot “run wild” and waste cellular resources.

PdhR regulation of *lipA* expression is problematical in that LipA is also required for activity of two other key *E. coli* proteins, the SucB subunit of the citric acid cycle 2-oxoglutarate dehydrogenase (OGDH) and the GcvH subunit of the glycine cleavage system (GCV) of single carbon metabolism [6, 5]. Therefore, if PdhR severely repressed *lipA* expression, these enzymes would be in their inactive octanoylated forms and thereby block metabolism. Although high pyruvate levels would reverse PdhR repression [33], placing the activity of two key enzyme systems, neither of which is directly involved in pyruvate metabolism, under regulation by pyruvate levels seemed physiologically incongruous. Indeed, the PDH, OGDH and GCV complexes have a common component, Lpd, which is the E3 subunit of the dehydrogenases and the L protein of GCV [7, 34]. Lpd expression is only partially regulated by PdhR in order to allow synthesis of functional OGDH and GCV. Two transcripts encode *lpd,* a read-through *pdhR-aceEF-lpd* polycistronic mRNA under PdhR control and a second monocistronic *lpd* transcript initiated from a promoter located in the region between *aceF* and *lpd* that does not bind PdhR [7]. The read-through transcript provides Lpd for PDH function whereas the monocistronic *lpd* transcript provides Lpd for the other two enzyme complexes. Hence, this transcription pattern acts to provide Lpd for each of the three enzyme complexes [7]. Since in the absence of exogenous lipoic acid, the growth phenotypes of *lipA* and *lpd* null mutant strains on glucose minimal media are

identical (supplementation with both acetate and succinate is required), strict PdhR regulation of *lipA* would mimic inactivation of *lpd*.

Other problems arise in the report of Kaleta and coworkers [24]. The publication reported no expression data and the electrophoretic mobility shift assay data show long trailing bands consistent with weak binding. Moreover, as described below the authors used an unusually large DNA probe *(ca.* 500 bp) that we found to contain three putatively weak PdhR binding sites. This raised the possibility that the reported mobility shift data represented weak binding to multiple sites rather than to the site chosen by the authors.

2. Materials and Methods

2.1. Bacterial strains and growth conditions

The bacterial strains (Table 1) were all *E. coli* K-12 derivatives and were grown aerobically at 37°C. The media were Luria-Bertani (LB) medium (10 g of tryptone, 5 g of yeast extract and 10 g of NaCl per liter; pH 7.5), rich broth (RB) medium; 10 g of tryptone, 1 g of yeast extract, and 5 g of NaCl per liter), or M9 minimal medium with either 4 mM oleate or 5 mM sodium acetate as the sole carbon source. When necessary, the concentrations of antibiotics were as follows (in μg/ml) sodium ampicillin, 100 and kanamycin sulfate, 25.

2,2. Plasmids and DNA manipulations

The *E. coli pdhR* sequence was PCR amplified using primers *pdhR*_ec-F plus *pdhR*_ec-R (Table 2) and ligated into the BamHI and XhoI sites of pET28a(+) expression vector to give plasmid 28a-*pdhR* (Table 1). The altered upstream region of *E. coli lipA* (referred to P*lipA*3D) was synthesized *in vitro* using overlap PCR [18]. The genomic DNA of *E. coli* MG1655 was the template used to amplify the 3′-end DNA fragment of the *lipA* promoter region with primers P*lipA*d-F3, P*lipA*d-F4 and P*lipA*d-R (Table 2), the resulting PCR products were used as templates for a second round of PCR amplification using the primer combination, P*lipA*d-F, P*lipA*d-F2 and P*lipA*d-R (Table 2); The final PCR amplification used the second round PCR products as templates using primers, P*lipA*d-F plus P*lipA*d-R to give the altered lipA upsteam region with SalI and EcoRI sites at the termini (Table 2). These sites were used for ligation first into vector pCR2.1 TOPO, and subsequently into the promoter-less integration pAH125 to give plasmid pAH-P*lipA*3D (Table 1). All plasmids were verified by both PCR assays and direct DNA sequencing.

2.3. Expression and purification of PdhR

E. coli BL21(DE3) carrying expression plasmid 28a-*pdhR* (Table 1) was induced with 0.5 mM isopropyl β-D-1-thiogalactopyranoside (IPTG) at 30°C for 3.5 h. Following two rounds of lysis in a French pressure cell, the bacterial supernatant was clarified by the removal of bacterial debris via centrifugation (30,966 x *g*, 30 min), and loaded onto a nickel chelate column (Qiagen). The column was washed with 1x PBS buffer containing 50 mM imidazole and the protein was eluted in buffer containing 150 mM imidazole. The protein was concentrated by ultrafiltration (30 kDa cut-off) and exchanged into phosphate buffered saline (pH 7.4) containing 10% glycerol. Purity of the N-terminal hexahistidine tagged recombinant PdhR protein was assayed by 12% SDS-PAGE [12, 15].

2.4. Chemical cross-linking assays

The solution structure of *E. coli* PdhR protein was addressed using chemical cross-linking with ethylene glycol bis-succinimidylsuccinate (Pierce) [19]. In each chemical cross-linking reaction (15 μl in total), the PdhR protein (~5 μM) was separately mixed with different concentrations of cross-linker (0, 5, 10, 20 and 20 μM), and incubated for one h at room temperature. All the reaction products were separated with 12% SDS-PAGE.

2.5. Liquid chromatography quadrupole time-of-flight mass spectrometry

The identity of the recombinant PdhR protein was verified using a Waters Q-Tof API-US Quad-ToF mass spectrometer linked to a Waters Nano Acquity UPLC [14]. The destained SDS-PAGE gel slice was digested with 25 μl of Sequencing Grade Trypsin (G-Biosciences, St. Louis, MO, 12.5 ng /μl in 25 mM ammonium bicarbonate) using a CEM Discover Microwave Digestor (Mathews, NC) for 15 min at 55°C and 50 W. The resultant peptides were extracte d with 50% acetonitrile containing 5% formic acids, dried using a Savant SpeedVac and suspended in 20 μl of 5% acetonitrile containing 0.1% formic acid. The sample (~10 μl) was loaded on a Waters Atlantis C-18 column (0.03 mm particle, 0.075 mm by 150 mm) and eluted at a flow rate of 250 nl per min using a linear gradient of water/ acetonitrile containing 0.1% formic acid 0–60% B in 60 min. Following data acquisition by the mass spectrometer, MS/MS analyses were conducted on the most abundant four peaks present at any given retention time. The Waters Protein Lynx Global Server 2.2.5, Mascot (Matrix Sciences) and the BLAST NCBI nr database was used for data processing [17, 14].

2.6. Electrophoretic mobility shift assays

The binding abilities of the putative PdhR-binding palindromes were evaluated using EMSA tests with minor modifications [20, 17, 14]. The digoxigenin (DIG)-labeled DNA probes were prepared *in vitro* through annealing two complementary oligonucleotides (Table 2) suspended in TEN buffer (10 mM Tris-HCl, 1 mM EDTA, 100 mM NaCl; pH 8.0) followed by the terminal transferase-aided labeling with DIG-ddUTP (Roche). The DNA probes were *lipA*1, *lipA*2 (which provided a negative control), *lipA*3, *lipA*3D (the constructed palindromic version of the *lipA*3 site) and *pdhR* (which provided a positive control) (Table 2). After 16 min of incubation of the DIG-labeled DNA probes (0.2 pmol) with or without PdhR in binding buffer (Roche) at room temperature, the DNA-protein complexes were separated using a native 7% PAGE gel, and the chemiluminescent signal captured by exposure to ECL film (Amersham) [15, 16].

2.7. $P1_{vir}$ phage transductions

$P1_{vir}$ transductions were done as in Miller [28]. Transduction of strain MC1061 with a lysate grown on FYJ198 (Δ*pdhR*::Km) with selection for kanamycin resistance gave strain FYJ429 (MC1061, Δ*pdhR*::Km). Subsequent expression of yeast FLP recombinase from plasmid pCP20 [9] removed the kanamycin resistance cassette to give strain FYJ433 (MC1061, Δ*pdhR*) which retaining a single FLP recombinase target (FRT) site (Table 1). Transductions of strains (FYJ201 (JW0109-1, Δ*lipA*) and FYJ203 (JW0109-1, Δ*pdhR*) with a $P1_{vir}$ lysate grown on FYJ204 (ZX226, *lipA-lacZ* fusion) with selection for kanamycin resistance gave strains FYJ215 (*lipA-lacZ* fusion) and FYJ209 (Δ*pdhR*, *lipA-lacZ* fusion), respectively

(Table 1). The *lipA-lacZ* fusion of strains FYJ215 and FYJ209 was constructed by Dr. Xin Zhao of this laboratory using the method of Ellermeier at al., [10]. The construct was verified by its *lipA* phenotype and sequencing of the PCR-derived chromosomal segment.

Strains FYJ430 and FYJ436 were constructed by transduction of strains MC1061 and FYJ433 (MC1061, Δ*pdhR*) with a $P1_{vir}$ lysate grown on FYJ215 (*lipA-lacZ* fusion) with selection for kanamycin resistance (Table 1). Similarly, the $P1_{vir}$ lysate grown on FYJ449 (MC4100, *lipA*3D-*lacZ* fusion) with selection for kanamycin resistance was transduced to strains MC1061 and FYJ443 (MC1061, Δ*pdhR*) giving the strains FYJ450 (MC1061, *lipA*3D-*lacZ* fusion), FYJ451 (MC1061, Δ*pdhR*, *lipA*3D-*lacZ* fusion), respectively (Table 1). All the relevant genotypes of the Δ*lipA* and Δ*pdhR* strains were verified using multiplex PCR with a primer set (either *lipA*-check- F/*lipA*-check2-F plus P*lipA*3D-R/*lacZ*-R or *pdhR*-check-F plus *pdhR*-check-R, Table 2). The PCR products were validated by direct DNA sequencing [16].

2.8. β-Galactosidase assays

The β-galactosidase activities were assayed using lysates from log-phase cultures obtained by treatment with sodium dodecyl sulfate-chloroform [27, 12].

2.9. Bioinformatic analyses

Multiple alignments were conducted using the ClustalW2 program (http://www.ebi.ac.uk/Tools/clustalw2/index.html) and final output was processed by the ESPript 2.2 server (http://espript.ibcp.fr/ESPript/cgi-bin/ESPript.cgi). The *lipA* regulons of γ-proteobacteria were collected from the RegPrecise database [30] and were analyzed [18] using RegPredict software [31].

3. Results and Discussion

3.1. Genetic context of lipA amongst β-proteobacteria

The pathway of lipoate synthesis in *E. coli* involves only two enzymes. LipB transfers an octanoyl moiety from octanoyl-ACP to a lipoyl domain of one of the cognate enzymes present on the E2 subunits of PDH and OGDH or GcvH. LipA then converts the covalently attached octanoyl moiety to lipoate by insertion of sulfur atoms at C6 and C8 using a radical mechanism dependent on S-adenosyl-L-methionine cleavage [5, 6]. Given that LipB and LipA catalyze two sequential steps and are specific to lipoate synthesis, cotranscription of *lipB* and *lipA* would be expected. Indeed in many -proteobacteria this seems to be the case although direct evidence of cotranscription is lacking. However, in *E. coli* and its close relatives, *lipB* and *lipA* are separated by a gene (*ybeF*) encoding a LysR-family transcription factor of unknown function (Fig. 2) and are not co-transcribed.

3.2. The E. coli lipA promoter

Mendoza-Vargas and coworkers [26] identified the *E. coli* K-12 *lipA* promoter in their high-throughput transcription initiation mapping experiments. Transcription is initiated 85 bp upstream of the coding sequence and is strongly conserved in γ-proteobacteria (Fig. 3A and B). In addition to the PdhR binding site predicted by Kaleta et al. [24] (referred to *lipA* site

1, located 61-77 bp downstream of the transcriptional initiation site), we also detected two other possible PdhR binding degenerate palindromes one downstream of the transcriptional initiation site (designated *lipA* site 2, 22 - 38 and another upstream of the initiation site (*lipA* site 3, −293 - −277) (Fig. 3B). All three of these sites are present in the EMSA probe of Kaleta and coworkers [24] and thus could contribute to the weak binding observed.

3.3. Characterization of E. coli PdhR protein

An N-terminal hexahistidine tagged *E. coli* PdhR protein was expressed in strain BL21(DE3) purified to homogeneity and the polypeptide gave single band of appropriate molecular mass on SDS-PAGE (Fig. 4A). Chemical crosslinking assays suggested that PdhR forms dimers at high concentration as expected from its binding to a palindromic sequence (Fig. 4B). PdhR was originally reported to be monomeric. However, the discrepancy may be more apparent than real because in the original report PdhR was found to be soluble only at very low concentrations (<50 μg/ml) which dictateed performing the gel filtration analysis under dilute conditions probably equivalent where we saw only traces of dimerization. (In our hands the tagged protein was much more soluble perhaps due to the hexahistidine tag.) Moreover, in the case of LexA protein [29] DNA binding has been shown to markedly stabilize the dimeric form and a similar situation might explain the apparent discrepancy between PdhR being predominately monomeric and the palindromic nature of its binding sites. Liquid chromatography mass spectrometry analyses of tryptic peptides of the putative PdhR protein band excised from an SDS-PAGE gel confirmed its identity in that the peptides matched *E. coli* PdhR with 74% coverage of the expected peptides (Fig. 4C).

3.4. Inefficient binding of PdhR to the DNA sequence upstream of E. coli lipA

The fact that the *lipA* upstream region DNA probe used by Kaleta et al in their EMSA assays was unusually long (~ 500 bp) [24] raised the possibility of weak binding of several sites by PdhR. Our sequence alignments of the putative PdhR boxes in the upstream region of *lipA* with known PdhR-binding palindromes suggested that *lipA* site 3 (CGTTTTTATAACCTGTT) was a better match than the *lipA* site1 (ATTCGCAACTGGAACA) predicted by Kaleta and coworkers (Fig. 3B and 5A). To test this hypothesis, we preformed EMSA analyses of the individual sites using a range of PdhR concentrations (Fig. 5). As anticipated, the PdhR (1–10 pmol) bound its own promoter (*pdhR* probe, Table 2) with good affinity and thereby provided a positive control (Fig. 5B). The *lipA* site 1 predicted by Kaleta et al. [24] failed to show any detectable binding by PdhR even at a level of 20 pmol (Fig. 5C). A very similar result was obtained for *lipA* site 2 (Fig. 3B and 5D). In contrast, the *lipA* site 3 exhibited a very modest binding affinity for PdhR protein although the probe was much more heavily labeled that the *pdhR* probe (compare Fig. 5B with 5E). Therefore, the site predicted by Kaleta et al. (*lipA* site 1) is not a functional PdhR binding site and their data can be attributed to PdhR binding of *lipA* site 3 (Fig. 3B and 5E). The weak PdhR binding of the *lipA* site 3 is consistent with the fact that it contains only half of the canonical PdhR palindrome (Fig. 5A and F) and engineering a palindrome into the *lipA* site 3 sequence resulted in much stronger PdhR binding (Fig. 5G – see below). Moreover, *lipA* site 3 (-277 - -293, Fig. 3B) is located much too far from the promoter to exert regulation of *lipA* transcription.

3.5. Lack of a regulatory role for PdhR in lipA expression

To test the physiological relevance of the above results *in vivo*, the *lipA* promoter was fused to a LacZ reporter gene to allow expression to be assayed by β-galactosidase activity (Table 1). Deletion of *pdhR* did not lead to any detectable change in *lipA* transcription level in LB medium (Fig. 6A). However, it remained possible that LB medium may contain sufficient pyruvate (or amino acids that are metabolized to pyruvate) that might inactivate PdhR, although in prior work high levels of pyruvate were added to LB in order to inactivate PdhR [23]. To test this possibility we assayed cultures grown in minimal medium on oleate or 5 mM acetate. Intracellular pyruvate levels vary greatly with carbon source with glucose giving the highest levels (0.9 μmol/g dry cell weight) and acetate the lowest (30-fold less than glucose) with succinate and glycerol giving values, respectively, 7 to 11-fold greater than acetate [25]. Acetate and oleate give the lowest intracellular pyruvate levels [2, 8, 25] because pyruvate must be made from acetyl-CoA using the glyoxylate cycle plus gluconeogenesis. In these pyruvate-limited cultures, *lipA* expression level in the Δ*pdhR* strain was slightly lower than that of the wild type strain (Fig. 6B and C) results generally consistent with the results seen in cultures grown in LB medium (Fig. 6A). Note that most of the *in vivo* work on PdhR has utilized glucose grown cells often in media also supplemented with pyruvate [23, 32, 33].

One possibility (other than chance) for the *lipA* 3 site is that this is a degenerating or developing regulatory system and that a high affinity site at the *lipA* 3 location might aid function of one or both of the weak *lipA* 1 and 2 sites by DNA looping. Therefore, we constructed a derivative of *lipA* site 3 (called *lipA*3D) having a perfect palindrome (Fig. 5F). As expected, EMSA experiments demonstrated that the *lipA*3D site bound PdhR with appreciably higher affinity (Fig. 5G) than did its parental *lipA* site 3 (Fig. 5E). By overlap PCR we replaced the *lipA* site 3 (Fig. 3B) with the *lipA*3D perfect palindrome construct (Fig. 5F) within the LipA promoter upstream sequence. This construct was fused to a pAH125 plasmid-borne *lacZ* reporter that was used to generate strain FYJ450 having a single chromosomal copy of the *lipA*3D-*lacZ* transcriptional fusion construct (Table 1). In this strain background, deletion of *pdhR* did not significantly alter *lipA*3D-*lacZ* transcription in cultures grown either LB medium (Fig. 6D) or with oleate as sole carbon source (Fig. 6E), but showed weak repression in cultures grown with acetate as sole carbon source (Fig. 6F). This suggests the possibility of a degenerating or developing regulatory system, although the differing results seen with oleate and acetate which both enter central metabolism as acetyl-CoA argue that this may be a secondary metabolic effect.

4. Conclusions

Our data demonstrate that the conclusion of Kaleta and coworkers [24, 21] that PdhR regulates *lipA* expression is incorrect.

Acknowledgments

This work was supported by National Institutes of Health Grant AI15650 (JEC) from the National Institute of Allergy and Infectious Diseases and a start-up package from Zhejiang University (YF). YF is a recipient of the “Young 1000 Talents” Award

References

1. Baba T, Ara T, Hasegawa M, Takai Y, Okumura Y, Baba M, Datsenko KA, Tomita M, et al. Construction of *Escherichia coli* K-12 in-frame, single-gene knockout mutants: the Keio collection. Mol Syst Biol. 2006; 2:2006–0008.
2. Barak Z, Chipman DM, Gollop N. Physiological implications of the specificity of acetohydroxy acid synthase isozymes of enteric bacteria. J Bacteriol. 1987; 169:3750–3756. [PubMed: 3301814]
3. Casadaban MJ, Cohen SN. Analysis of gene control signals by DNA fusion and cloning in *Escherichia coli*. J Mol Biol. 1980; 138:179–207. [PubMed: 6997493]
4. Cherepanov PP, Wackernagel W. Gene disruption in *Escherichia coli*: TcR and KmR cassettes with the option of Flp-catalyzed excision of the antibiotic-resistance determinant. Gene. 1995; 158:9–14. [PubMed: 7789817]
5. Cronan, J. Biotin and Lipoic Acid: Synthesis, Attachment, and Regulation. In: Stewart, V.; Begley, T., editors. EcoSal Plus 2014. 2014.
6. Cronan JE, Zhao X, Jiang Y. Function, attachment and synthesis of lipoic acid in *Escherichia coli*. Adv Microb Physiol. 2005; 50:103–146. [PubMed: 16221579]
7. Cunningham L, Georgellis D, Green J, Guest JR. Co-regulation of lipoamide dehydrogenase and 2-oxoglutarate dehydrogenase synthesis in *Escherichia coli*: characterisation of an ArcA binding site in the lpd promoter. FEMS Microbiol Lett. 1998; 169:403–408. [PubMed: 9868788]
8. Dailey FE, Cronan JE Jr. Acetohydroxy acid synthase I, a required enzyme for isoleucine and valine biosynthesis in *Escherichia coli* K-12 during growth on acetate as the sole carbon source. J Bacteriol. 1986; 165:453–460. [PubMed: 3511034]
9. Datsenko KA, Wanner BL. One-step inactivation of chromosomal genes in *Escherichia coli* K-12 using PCR products. Proc Natl Acad Sci U S A. 2000; 97:6640–6645. [PubMed: 10829079]
10. Ellermeier CD, Janakiraman A, Slauch JM. Construction of targeted single copy *lac* fusions using lambda Red and FLP-mediated site-specific recombination in bacteria. Gene. 2002; 290:153–161. [PubMed: 12062810]
11. Feng Y, Cronan JE. *Escherichia coli* unsaturated fatty acid synthesis: complex transcription of the *fabA* gene and *in vivo* identification of the essential reaction catalyzed by FabB. J Biol Chem. 2009; 284:29526–29535. [PubMed: 19679654]
12. Feng Y, Cronan JE. A new member of the *Escherichia coli fad* regulon: transcriptional regulation of *fadM* (*ybaW*). J Bacteriol. 2009; 191:6320–6328. [PubMed: 19684132]
13. Feng Y, Cronan JE. Overlapping repressor binding sites result in additive regulation of *Escherichia coli* FadH by FadR and ArcA. J Bacteriol. 2010; 192:4289–4299. [PubMed: 20622065]
14. Feng Y, Cronan JE. Complex binding of the FabR repressor of bacterial unsaturated fatty acid biosynthesis to its cognate promoters. Mol Microbiol. 2011; 80:195–218. [PubMed: 21276098]
15. Feng Y, Cronan JE. The *Vibrio cholerae* fatty acid regulatory protein, FadR, represses transcription of *plsB*, the gene encoding the first enzyme of membrane phospholipid biosynthesis. Mol Microbiol. 2011; 81:1020–1033. [PubMed: 21771112]
16. Feng Y, Cronan JE. Crosstalk of *Escherichia coli* FadR with global regulators in expression of fatty acid transport genes. PLoS One. 2012; 7:e46275. [PubMed: 23029459]
17. Feng Y, Napier BA, Manandhar M, Henke SK, Weiss DS, Cronan JE. A *Francisella* virulence factor catalyses an essential reaction of biotin synthesis. Mol Microbiol. 2014; 91:300–314. [PubMed: 24313380]
18. Feng Y, Xu J, Zhang H, Chen Z, Srinivas S. *Brucella* BioR regulator defines a complex regulatory mechanism for bacterial biotin metabolism. J Bacteriol. 2013; 195:3451–3467. [PubMed: 23729648]
19. Feng Y, Zhang H, Cronan JE. Profligate biotin synthesis in alpha-proteobacteria - a developing or degenerating regulatory system? Mol Microbiol. 2013; 88:77–92. [PubMed: 23387333]
20. Goble AM, Feng Y, Raushel FM, Cronan JE. Discovery of a cAMP deaminase that quenches cyclic AMP-dependent regulation. ACS Chem Biol. 2013; 8:2622–2629. [PubMed: 24074367]

21. Gohler AK, Kokpinar O, Schmidt-Heck W, Geffers R, Guthke R, Rinas U, Schuster S, Jahreis K, et al. More than just a metabolic regulator--elucidation and validation of new targets of PdhR in *Escherichia coli*. BMC Syst Biol. 2011; 5:197. [PubMed: 22168595]
22. Haldimann A, Wanner BL. Conditional-replication, integration, excision, and retrieval plasmid-host systems for gene structure-function studies of bacteria. J Bacteriol. 2001; 183:6384–6393. [PubMed: 11591683]
23. Haydon DJ, Quail MA, Guest JR. A mutation causing constitutive synthesis of the pyruvate dehydrogenase complex in *Escherichia coli* is located within the *pdhR* gene. FEBS Lett. 1993; 336:43–47. [PubMed: 8262214]
24. Kaleta C, Gohler A, Schuster S, Jahreis K, Guthke R, Nikolajewa S. Integrative inference of gene-regulatory networks in *Escherichia coli* using information theoretic concepts and sequence analysis. BMC Syst Biol. 2010; 4:116. [PubMed: 20718955]
25. Lowry OH, Carter J, Ward JB, Glaser L. The effect of carbon and nitrogen sources on the level of metabolic intermediates in *Escherichia coli*. J Biol Chem. 1971; 246:6511–6521. [PubMed: 4257200]
26. Mendoza-Vargas A, Olvera L, Olvera M, Grande R, Vega-Alvarado L, Taboada B, Jimenez-Jacinto V, Salgado H, et al. Genome-wide identification of transcription start sites, promoters and transcription factor binding sites in *E. coli*. PLoS One. 2009; 4:e7526. [PubMed: 19838305]
27. Miller, J. Experiments in Molecular Genetics. Cold Spring Harbor, NY: Cold Spring Harbor Laboratory Press; 1972.
28. Miller, JH. A short course in bacterial genetics. Cold Spring Harbor Laboratory; Cold Spring Harbor, N.Y: 1992.
29. Mohana-Borges R, Pacheco AB, Sousa FJ, Foguel D, Almeida DF, Silva JL. LexA repressor forms stable dimers in solution. The role of specific dna in tightening protein-protein interactions. J Biol Chem. 2000; 275:4708–4712. [PubMed: 10671501]
30. Novichkov PS, Laikova ON, Novichkova ES, Gelfand MS, Arkin AP, Dubchak I, Rodionov DA. RegPrecise: a database of curated genomic inferences of transcriptional regulatory interactions in prokaryotes. Nucleic Acids Res. 2010; 38:D111–118. [PubMed: 19884135]
31. Novichkov PS, Rodionov DA, Stavrovskaya ED, Novichkova ES, Kazakov AE, Gelfand MS, Arkin AP, Mironov AA, et al. RegPredict: an integrated system for regulon inference in prokaryotes by comparative genomics approach. Nucleic Acids Res. 2010; 38:W299–307. [PubMed: 20542910]
32. Ogasawara H, Ishida Y, Yamada K, Yamamoto K, Ishihama A. PdhR (pyruvate dehydrogenase complex regulator) controls the respiratory electron transport system in *Escherichia coli*. J Bacteriol. 2007; 189:5534–5541. [PubMed: 17513468]
33. Quail MA, Haydon DJ, Guest JR. The *pdhR-aceEF-lpd* operon of *Escherichia coli* expresses the pyruvate dehydrogenase complex. Mol Microbiol. 1994; 12:95–104. [PubMed: 8057842]
34. Spencer ME, Guest JR. Transcription analysis of the *sucAB*, *aceEF* and *lpd* genes of *Escherichia coli*. Mol Gen Genet. 1985; 200:145–154. [PubMed: 3897791]

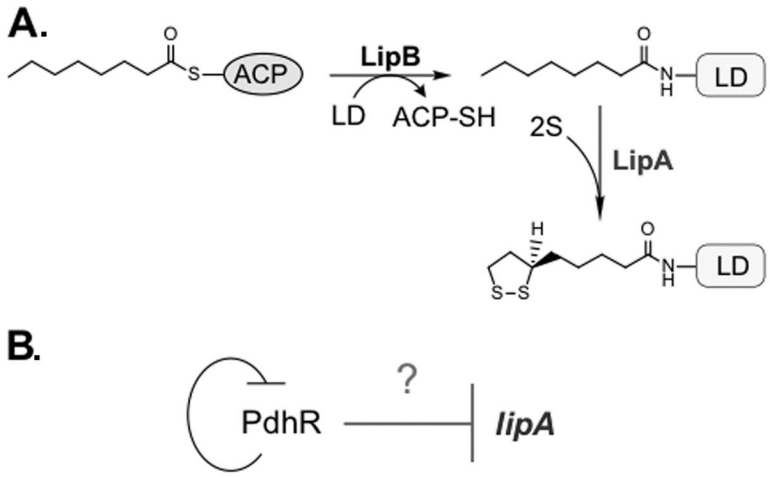

Figure 1. Pathway for lipoic acid metabolism and its putative regulation in *E. coli*

(A) Pathways for *de novo* biosynthesis of lipoic acid and its scavenging in *E. coli*. LipA, lipoic acid synthase; LipB, Octanoyl-ACP: protein ligase (N-octanoyltransferase); PdhR, pyruvate dehydrogenase operon repressor; LD, lipoyl domain (in pink); ACP, Acyl carrier protein (in light blue).

(B) The model proposed for negative regulation of *lipA* by the auto-regulated repressor PdhR [23].

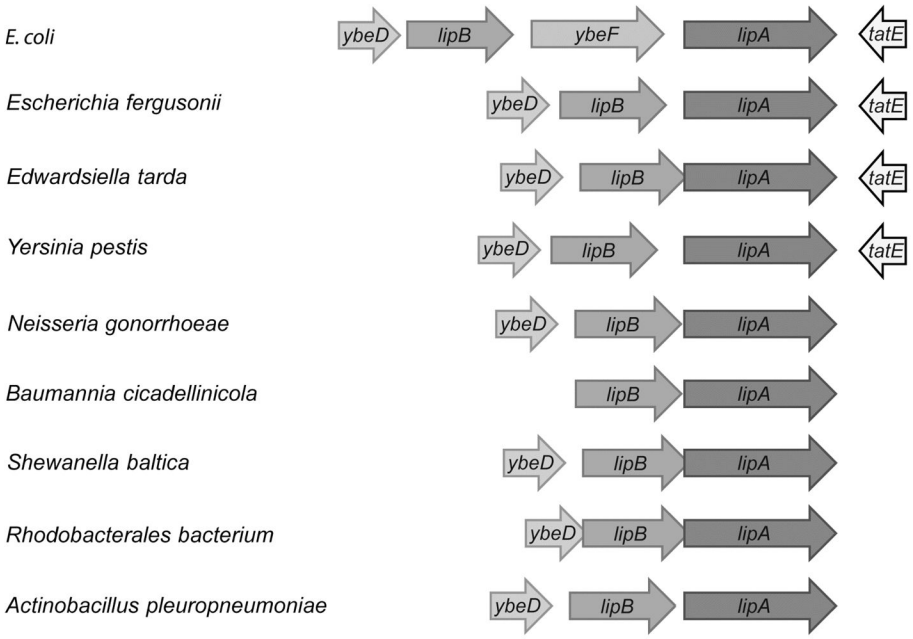

Figure 2. Diversity of lipoic acid synthesis genes in *β-proteobacteria*

The *lipA* genes that encode lipoic acid synthase are represented with blue arrows whereas the octanoyl-protein ligase *lipB* genes are indicated with green arrows. In most species, *ybeD*, a gene of unknown function is located upstream of the *lipB* gene (grey arrows) whereas the *tatE* (Sec-independent protein translocase) encoded downstream of *lipA* is in yellow. In some cases, a LysR-family transcription factor-encoding gene *ybeF* is located *lipA* between *lipB* is highlighted (orange).

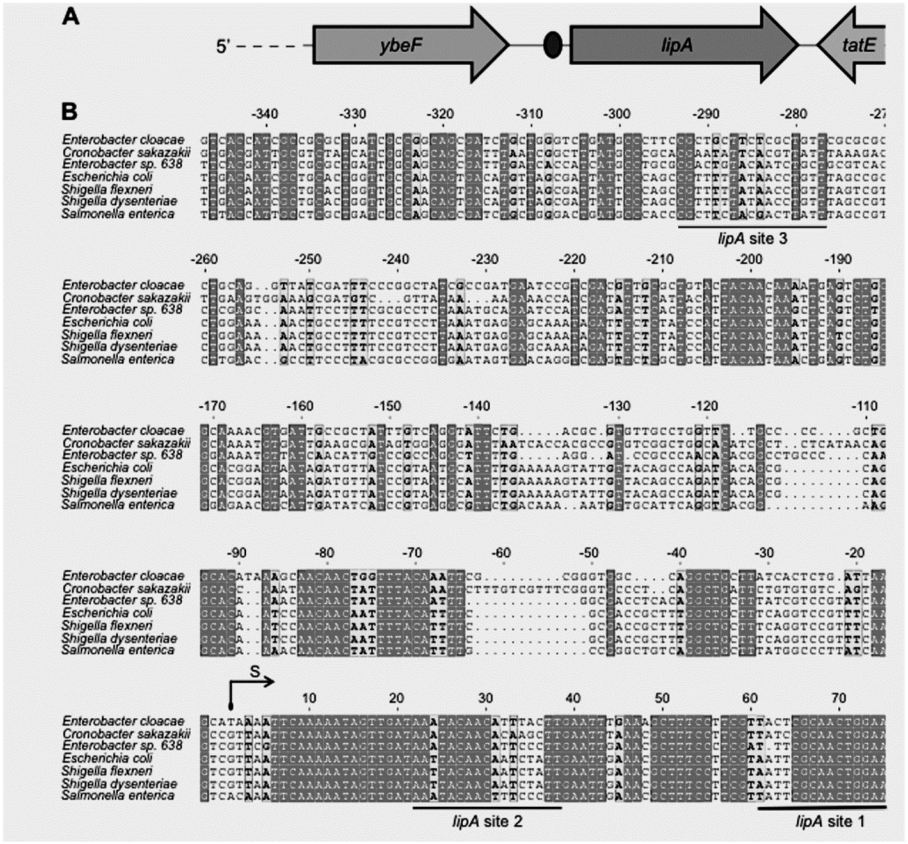

Figure 3. Sequence analyses of *lipA* promoters

(A) Cartoon depiction of the genome neighborhood of *E. coli lipA.*

The oval of Panel A denotes the putative PdhR-binding site of Kaleta and coworkers [23] which is *lipA* site 1 of Panel B

(B) Multiple sequence alignments of *lipA* promoters of seven *β-proteobacterial* species

The *lipA* promoter sequences of seven organisms used here are derived from *Escherichia coli* (U00096.3), *Enterobacter cloacae* (CP002886.1), *Enterobacter sp. 638* (CP000653.1), *Cronobacter sakazakii* (YP_006343855.1), *Shigella flexneri* (AAN42289.1), *Shigella dysenteriae* (EDX35164.1) and *Salmonella enterica* (NP_459625.1), respectively, aligned with ClustalW2 (http://www.ebi.ac.uk/Tools/clustalw2/index.html) and tprocessed with ESPript 2.2 (http://espript.ibcp.fr/ESPript/cgi-bin/ESPript.cgi) [18, 12, 13]. Identical bases are indicated with white letters on a dark gray background, similar bases are bold letters on a light gray background, variable residues are in black letters and dots represent missing residues. The reported PdhR-recognized palindrome upstream of *lipA* gene (designated *lipA* site 1) [24] and the other two predicted sites are underlined in black. Abbreviations: S, transcription start site [26].

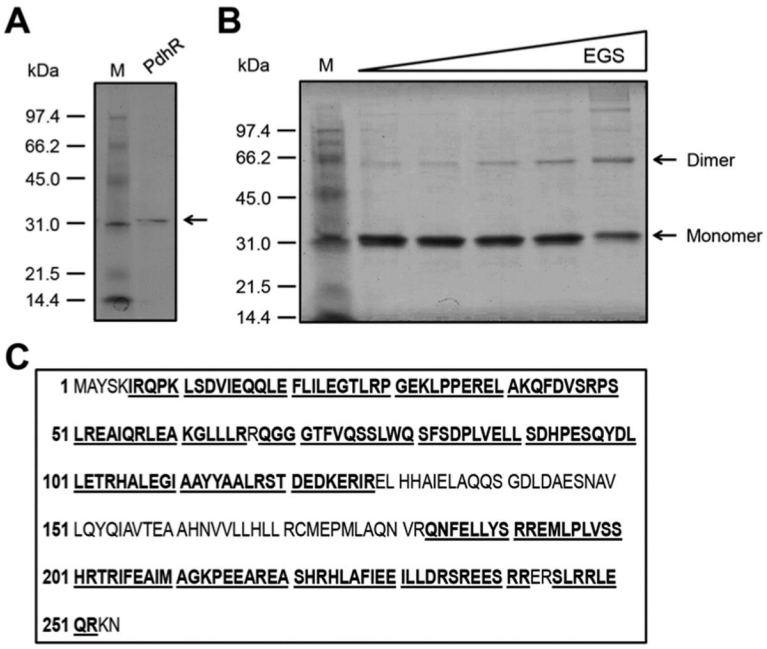

Figure 4. Preparation, identification and characterization of PdhR

(A) SDS-PAGE (12%) analysis of purified PdhR.

The molecular weights of the standard protein markers (Biorad) are labeled at the left. The N-terminal tagged PdhR protein with an expected size (~32 kDa) is indicated by an arrow.

(B) Chemical cross-linking assays for the solution structure of the PdhR protein.

Ethylene glycol bis-succinimidylsuccinate (EGS) was the cross-linker. The triangle on the top represents the addition of EGS cross linker in varied concentrations (0, 5, 10, 20, 50 μM in the right-hand five lanes [left to right]). M: Molecular weight. The monomeric PdhR protein size is predicted to be ~32 kDa, and thus the dimeric weight is ~64 kDa.

(C) MS identification of the purified PdhR protein

The tryptic peptides with hits to the PdhR sequence are given in bold underlined type.

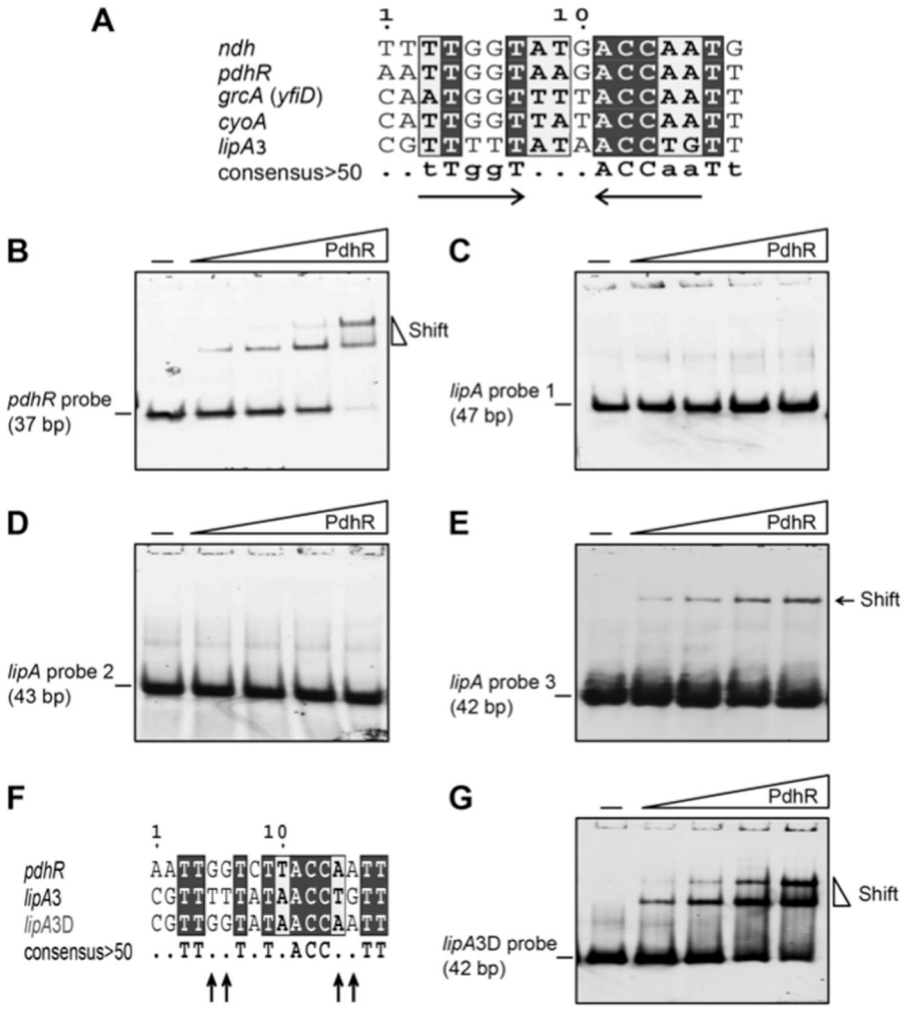

Figure 5. EMSA analyses of PdhR binding of *E. coli lipA* upstream sequences

A. Sequence alignment of the putative PdhR binding site (*lipA*3) predicted by Kaleta and coworkers [24].

(B) Binding of PdhR to its promoter autoregulatory site.

(C) Binding of PdhR to *lipA* probe 1.

(D) Binding of PdhR to *lipA* probe 2 (negative control).

(E) Binding of PdhR to *lipA* probe 3.

(F) Sequence comparison of the constructed PdhR perfect palindrome derived from the *lipA3* site (referred to *lipA*3D) known *pdhR* binding site.

(G) Binding of PdhR to the *lipA*3D site.

The sequence alignments are depicted as in Fig. 3. The PdhR binding site palindrome is indicated by the two inverted arrows. Dots represent bases with less than 50% consensus and the altered bases are highlighted with arrows. The PdhR concentrations of (B, D, and E) [left to right]) were 0.05, 0.1, 0.25, and 0.5 μM, whereas in the right-hand four lanes of C & G [left to right]) the concentrations were 0.1, 0.25, 0.5, and 1 μM. The protein samples were incubated with 0.01 μM of DIG-labeled probe (in Table 2) in a total volume of 20 μl. The

gel shift experiments are conducted with 7% native PAGE. A representative result of more than three independent experiments is given.

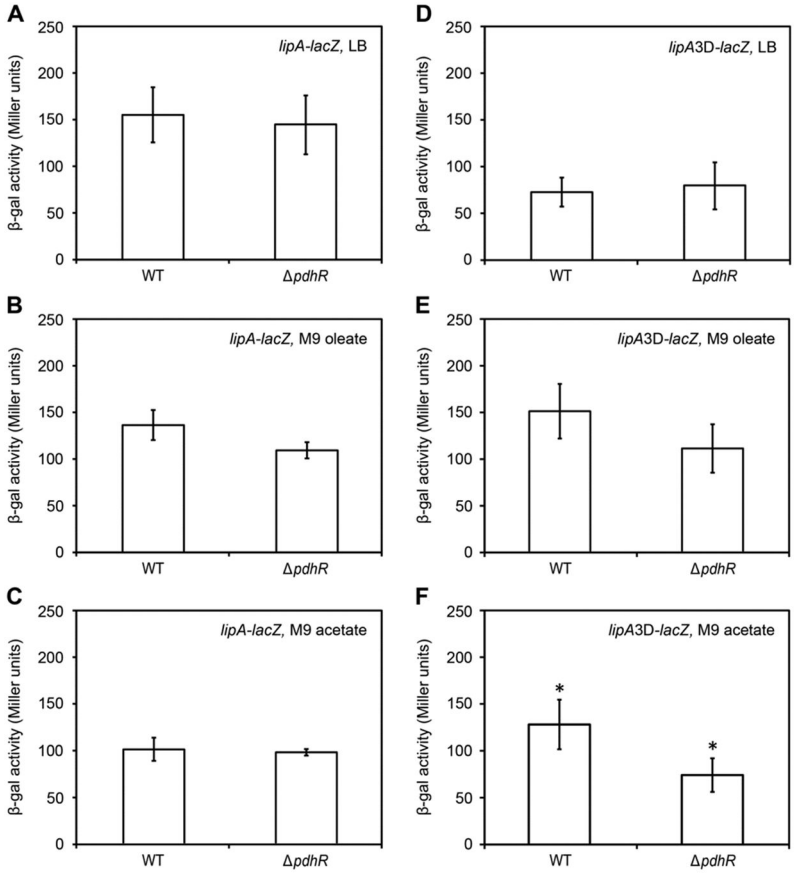

Figure 6. Lack of PdhR regulation of *lipA* and *lipA*3D transcription *in vivo*

(A-C) β-Galactosidase production from the *lipA-lacZ* fusion in cultures grown on LB medium (A), oleate minimal medium (B) or acetate minimal medium (C). In the *lipA-lacZ* transcriptional fusion, expression of the promoter-less *lacZ* cassette is driven by the native *lipA* promoter. The strain has a *lipA* phenotype. (D-E) β-Galactosidase production from the *lipA*3D-*lacZ* fusion in cultures grown on LB medium (D), oleate minimal medium (E) or acetate minimal medium (F), but give weak activation for expression of on the condition of minimal media M9 with acetate as sole carbon source (F). The data are expressed in the average ± SD (*P<0.001). Three or more independent experiments were performed. The *E. coli* strains carrying *lipA- lacZ* transcriptional fusions were FYJ430 (MC1061, *lipA-lacZ*) and FYJ436 (MC1061, Δ*pdhR*, *lipA-lacZ*), whereas the strains with the engineered *lipA*3D-*lacZ* fusions were FYJ450 (WT) and FYJ451 (Δ*pdhR*) The *lipA*3D carries a version of the *lipA*3 site (CGTTTT TAT AACCTGTT, bp 335 to 351) converted two a typical palindrome *lipA*3D site (CGT TGG TAT AACCAATT with changes underlined). The lacZ fusion to this promoter was constructed on a suicide plasmid which was integrated into the *attB* site of phage λ. The medium used in (A & D) was LB supplemented with 2 μM succinate/acetate to bypass the lipoic acid requirement. To minimize intracellular pyruvate levels the minimal medium M9 containing either 4 mM oleate or 5 mM sodium acetate as sole carbon source was used.

Table 1

Strains and plasmids used in this study

Strains or plasmids	Relevant characteristics	Ref or origin
***E. coli* Strains**		
Topo10	cloning *h*ost (F^-, Δ*lac*X74)	Invitrogen
BL21(DE3)	Expression host	Lab stock
DH5α(λ-*pir*)	Δ*lac* host for pAH125 and its derivatives	[11, 16, 22]
MC4100	(*araD*139, Δ (*argF*-*lac*)169)	[12]
MG1655	Wild type	CGSC[a], Lab stock
BW25113	Δ*lac* Δ *(araD-araB)567*, Δ*lacZ4787*(::rrnB- 3), Δ (*rhaD-rhaB*)*568*, *hsdR514*)	CGSC[a], [1]
FYJ198	JW0109-1(BW25113, Δ*pdhR::*Km)	CGSC[a], [1]
MC1061	Δ (*araA-leu*)7697 [*araD139*]$_{B/r}$, Δ (*codB- lacI*)*3*, *galK16*, *galE15*(*GalS*), *e14*$^-$, *mcrA0*, *relA1*, *rpsL150*(strR), *spoT1*, *mcrB1*, *hsdR2*	Lab stock, [3]
FYJ187	MC4100 carrying pINTts	[15]
FYJ199	JW0623-1(BW25113, Δ*lipA*::Km)	CGSC[a], [1]
FYJ200	JW0109-1 carrying pCP20ts	This work
FYJ201	FYJ199 (Δ*lipA*::Km) carrying pCP20ts	This work
FYJ203	JW0109-1, Δ*pdhR*	This work
FYJ204	ZX226A (JK1, *lipA-lacZ* transcriptional fusion)	Lab stock
FYJ209	FYJ203 (Δ*pdhR*), *lipA-lacZ* transcriptional fusion	P1$_{vir}$(FYJ204)×FYJ203[b], This work
FYJ211	BL21(DE3) carrying 28-*pdhR*	This work
FYJ215	FYJ201, *lipA-lacZ* transcriptional fusion	P1$_{vir}$(FYJ204)×FYJ201[b], This work
FYJ429	MC1601, Δ*pdhR*::Km	P1$_{vir}$(FYJ198)×MC1061[b], This work
FYJ430	MC1061, *lipA-lacZ* transcriptional fusion	P1$_{vir}$(FYJ215)×MC1061[b], This work
FYJ433	MC1061, Δ*pdhR*	This work
FYJ436	FYJ433 (MC1061, Δ*pdhR*), *lipA-lacZ* transcriptional fusion	P1$_{vir}$(FYJ215)×FYJ433[b], This work
FYJ477	Topo10 carrying pCR-P*lipA*3D	This work
FYJ488	DH5α(λ-*pir*) carrying pAH-*PlipA*3D	This work
FYJ449	MC4100, *lipA*3D-*lacZ* transcriptional fusion	This work
FYJ450	MC1061, *lipA*3D-*lacZ* transcriptional fusion	P1$_{vir}$(FYJ449)×MC1061[b], This work
FYJ451	FYJ443 (MC1061, Δ*pdhR*), *lipA*3D-*lacZ* transcriptional fusion	P1$_{vir}$(FYJ449)×FYJ443[b], This work
Plasmids		
pCR2.1	High copy Topo-cloning vector, Amp^R Km^R	Invitrogen
pET28(a)	Commercial T7-driven expression vector, Km^R	Novagen
pINTts	Temperature sensitive plasmid expressing phage λ Int., Amp^R	[22]
pCP20	A temperature-sensitive plasmid encoding yeast FLP recombinase	[4, 10, 9]
pAH125	A promoter-less *lacZ* reporter plasmid used in *E. coli*, Kan^R	[11, 16, 22]
28a-*pdhR*	pET28(a) carrying *E. coli pdhR* gene, Km^R	This work
pCR-P*lipA*3D	pCR2.1 encoding the mutated promoter P*lipA*3D for *E. coli lipA* gene	This work

Strains or plasmids	Relevant characteristics	Ref or origin
pAH-P*lipA*3D	pAH125 encoding the mutated promoter P*lipA*3D for *E. coli lipA* gene	This work

[a] CGSC denotes Coli Genetic Stock Center, Yale University;

[b] Selection for kanamycin resistance

Table 2

DNA oligonucleotides used in this study

Oligonucleotide	Sequence
*pdhR*_ec-F	5′-CG *GGATCC* ATG GCC TAC AGC AAA ATC CG-3′
*pdhR*_ec-R	5′-CCG *CTCGAG* CTA ATT CTT TCG TTG CTC CAG-3′
*pdhR*_site-F (37 bp)	5′-GCC GAA GTC **AAT TGG TCT TAC CAA TT**T CAT GTC TGT G-3′
*pdhR*_site-R	5′-CAC AGA CAT GA**A ATT GGT AAG ACC AAT T**GA CTT CGG C-3′
*lipA*_site1-F (-8~ - 28) (47 bp)	5′-GAA ACG CTT TCC TTC GT**A ATT CGC AAC TGG AAC A**CG CAC GCT ATG AG-3′
*lipA*_site1-R	5′-CTC ATA GCG TGC G**TG TTC CAG TTG CGA ATT ACG A**AG GAA AGC GTT TC-3′
*lipA*_site2-F (-47~- 63) (43 bp)	5′-CAA AAA TAG TTG AT**A ATT ACA ACA ATC TAT T**GA ATT GAA ACG C-3′
*lipA*_site2-*R*	5′-GCG TTT CAA TTC **AAT AGA TTG TTG TAA TT**A TCA ACT ATT TTT G-3′
*lipA*_site3-F (-335 ~ -351) (42 bp)	5′-GAT TAT TCC CAG C**CG TTT TTA TAA CCT GTT** TAG CCG CTG CTG-3′
*lipA*_site3-R	5′-CAG CAG CGG CTA **AAC AGG TTA TAA AAA CG**G CTG GGA ATA ATC-3′
lipA-check-F	5′-CCA ACA GTG ACA TGT TAG CG-3′
lipA-check2-F	5′-CCA ACT CAG TCA GTT TCA AAC-3′
lacZ-R	5′-CAG TGA ATC CGT AAT CAT GGT C-3′
pdhR-check-F	5′-GCG TCA CAG ACA TGA AAT TGG-3′
pdhR-check-R	5′-GCA AGC AGT TGG TCG ATC AG-3′
*lipA*_site3d-F	5′-GAT TAT TCC CAG C**CG TTG GTA TAA CCA ATT** TAG CCG CTG CTG-3′
*lipA*_site3d-R	5′-CAG CAG CGG CTA **AAT TGG TTA TAC CAA CG**G CTG GGA ATA ATC-3′
P*lipA*d-F (SalI)	5′-CCG *GTCGAC* GTT AGC GAT TAT TCC CAG CC**G TTG GTA TAA CCA ATT** TAG CCG-3′
P*lipA*d-F2	5′-CC**G TTG GTA TAA CCA ATT** TAG CCG CTG CTG GCC GCT GGA AAA ACT GCC TTT TCC-3′
P*lipA*d-F3	5′-GCC GCT GGA AAA ACT GCC TTT TCC GTC CTT AAA TGA GGA GC-3′
P*lipA*d-F4	5′-CCG TCC TTA AAT GAG GAG CA-3′
P*lipA*d-R (EcoRI)	5′-AACC *GAATTC* CAT AGC GTG CGT GTT CCA GT-3′

The restriction sites are underlined and putative PdhR binding sites are in bold.